Desalination and Water Treatment
www.deswater.com

doi: 10.5004/dwt.2022.29034

277 (2022) 234–243
November

Optimization and kinetic evaluation of reactive yellow dye degradation by solar photocatalytic process

Noor A Mohammed[a], Abeer I. Alwared[a,*], Maryam Jawad Abdulhasan[b], Mohammed Sadiq Salman[c]

[a]*Department of Environmental Engineering, College of Engineering, University of Baghdad, Iraq, emails: dr.abeer.wared@coeng.uobaghdad.edu.iq (A.I. Alwared), noor.mohammed1211@coeng.uobaghdad.edu.iq (N.A. Mohammed)*
[b]*Chemical Engineering and Petroleum Industries Department, Al-Mustaqbal University College, Babylon, Iraq, email: maryam.jawad@mustaqbal-college.edu.iq*
[c]*Avi-Cenna E-learning Center, University of Baghdad, Iraq, email: m.sadiq@uobaghdad.edu.iq*

Received 4 May 2022; Accepted 10 October 2022

ABSTRACT

Response surface methodology (RSM) was applied based on the central composite design to find the optimum parameters for the degradation of reactive yellow (RY) dye in an aqueous solution using a solar-induced photocatalytic process. The independent variables considered were pH, TiO_2, H_2O_2, initial RY dye concentration, and irradiation time. Optimization of parameters was performed by analysis of variance (ANOVA). In addition, a polynomial multiple regression equation was suggested as a model for the prediction of RY dye elimination percentage. The results show that the RY dye removal at the optimal conditions of pH 6.95294, TiO_2 concentration 25.5441 mg/L, H_2O_2 concentration 383.676 mg/L, RY initial dye concentration 20.9412 mg/L, and irradiation time 89.6176 min was 91%. The ANOVA presents the coefficients of determination were R^2 = 0.9259 and R^2_{adj} = 0.9147, which confirm a satisfactory adjustment of the second-order regression model with the achieved data. Also, the results confirm that the removal percentage of RY dye follows a pseudo-first-order kinetic model with $R^2 > 0.92$. This study suggests that sunlight, catalyst, and H_2O_2 together have a significant effect on the degradation process, and under optimum operating conditions have a reasonable efficiency in the degradation of RY dye. Further, RSM was a suitable technique for the optimization of the variables involved in RY dye removal through the photocatalytic process.

Keywords: Reactive yellow dye; Solar photocatalysis; Kinetic model; Response surface methodology; Desirability function

1. Introduction

Environmental pollution is an alarming problem in developing countries. The textile industry is one of the largest and rapidly developing industries in the world. A dye is a colored substance used in many industries such as the textile industry, leather, cosmetics, paints, food, ceramics, construction wax, and paper. Environmental problems such as water and soil pollution are mainly due to the release of untreated textile dyes from the industries, surface runoffs, and sewage leakage and overflows [1]. Dyeing compounds are made up of synthetic organic molecules with a complicated molecular structure and a large molecular weight, allowing them to be used as dyes. The existence of dyes in the wastewater of the textile industry is not only visible but results in photosynthesis and aquatic life deterioration (even at low concentrations), owing to the carcinogenic nature of the dyes and their break-down products

* Corresponding author.

[2]. This may be explained by the presence of aromatic amines produced after the biodegradation of azo dyes [3]. Dyes are classified into different types, according to the process of dying: acid, basic, mordant, direct, reactive, vat, disperse, sulphur, and azo dyes [4]. Reactive dyes are synthetic, organic, colorant compounds, which are widely used as colorant agents in several manufacturing activities [5]. Reactive yellow (RY) dye is one of the reactive textile dyes largely used in textile finishing processes. Therefore, their removal from wastewater has major importance and needs to be done before it can be discharged to surface water [6]. Reactive dye effluents are not easy to treat by conventional treatment technologies, such as coagulation/flocculation [7], and electrocoagulation [8]. This is due to the fact that dye molecules are characterized as highly soluble, recalcitrant, and low biodegradable elements that resist the conventional treatment processes [6]. Therefore, numerous physicochemical methods such as precipitation, coagulation, flocculation, and photodegradation [9] and adsorption [10] have been used to remove dyes from aqueous solutions. Among them, advanced oxidation processes (AOPs) are known as the proper technique for decolorization of textile effluents and turning them into less harmful ones by generating hydroxyl with high oxidation potential [11,12]. Heterogeneous AOPs in which semiconductor solid photocatalysts are activated under UV or visible light are used in AOPs; they are simple, clean, effective, and cost-effective processes compared to other AOPs and their mechanism reaction can be described by Eqs. (1)–(7) [13,14]:

$$\text{Photocatalysts} + h_v \rightarrow e^- + h^+ \quad (1)$$

$$h^+ + H_2O \rightarrow H^+ + OH^- \quad (2)$$

$$h^+ + OH^- \rightarrow OH^\bullet \quad (3)$$

$$e^- + O_2 \rightarrow O_2^- \quad (4)$$

$$2e^- + O_2 + 2H^+ \rightarrow H_2O_2 \quad (5)$$

$$e^- + H_2O_2 \rightarrow OH^\bullet \rightarrow OH^- \quad (6)$$

$$\text{Organic} + {}^\bullet OH + O_2 \rightarrow CO_2 \rightarrow H_2O \quad (7)$$

To date, numerous semiconductor photocatalysts such as TiO_2, ZnO, C_3N_4, and $SrTiO_3$ have been investigated. However, TiO_2 is still considered a suitable photocatalyst due to its high chemical stability, low-cost, and environmentally friendly [15].

The minimum bandgap energy necessary for photons to cause charge carrier photo generation over anatase TiO_2 is 3.2 eV, which corresponds to λ = 388 nm. The energy corresponding to this wavelength is available from solar light; hence solar light is the potential source to generate charge carriers over TiO_2 [16]. The use of natural solar UV energy (sunlight), instead of the artificial UV lamp, may help greatly in reducing the cost of photocatalytic oxidation in relation to some alternative technologies [17,18].

In recent years, various statistical methods have been reported for optimizing variables, one of which is the response surface methodology (RSM). The RSM is a powerful statistical tool for describing the interactions between dependent (target) and independent (inputs) variables in this case [19,20], it consists of a group of mathematical and statistical techniques based on the fit of a polynomial equation to the experimental data in order to predict the behavior of a system and to reduce time and costs [21]. There are many methods to optimize the processes such as Box–Behnken design, face centered design (FCD), and central composite design (CCD). Among these methods, CCD was applied, due to its simple structure and good efficiency.

In the last few years, RSM has been applied to optimize and evaluate the interactive effects of independent factors in numerous chemical and biochemical processes such as adsorption [22], flotation [23], emulsion liquid membrane [24], and photocatalysis systems [25]. The objective of this study was to obtain the significant parameters affecting the photocatalytic degradation with the assistance of H_2O_2 for RY dye under solar light irradiation and further optimize the responses to maximize the efficiency of the process using the RSM method.

2. Materials and method

2.1. Reagents

The commercial RY dye obtained from the Al-Kut Textile Industry, (Department of Dying and Printing, Iraq) was selected as a dye pollutant model. In addition, TiO_2-P25 as powder supplied by Fluka (China) with 99% purity, molecular weight 79.87 g/mol and hydrogen peroxide obtained from Merck were used. The pH of the aqueous dye solution has been controlled through the experiments to the specified value by using (0.1 M) HCl and/or NaOH.

2.2. Procedure and analysis

The photocatalytic experiments were conducted on sunny days from July to October 2020 between (11 am and 2 pm) in a batch-mode reactor. The experiments were conducted in an open Pyrex glass of (600 mL) capacity that had been sprayed with silver nitrate to operate as a good solar reflector [26] and contained a piece of the mirror at the bottom (used as a reflector), Fig. 1. However, solar radiation was measured using the (SPM-1116SD). The device was directed toward the sun to measure the solar radiation that reaches the reactor. UV measurements were obtained for the range 300 and 400 nm with an average solar UV power of 150–850 W/m^2. A stock solution of RY dye was arranged by dissolving a suitable amount of RY dye in distilled water, then the required concentration 25, 50, 75, and 100 mg/L was prepared and then pH was adjusted before adding the reagents by using pH meter (WTW, INOLAB72, Germany). Subsequently, the desired concentration of TiO_2 was added, then the desired concentration of H_2O_2 was introduced to the reaction. The suspension was stirred at 200 rpm with

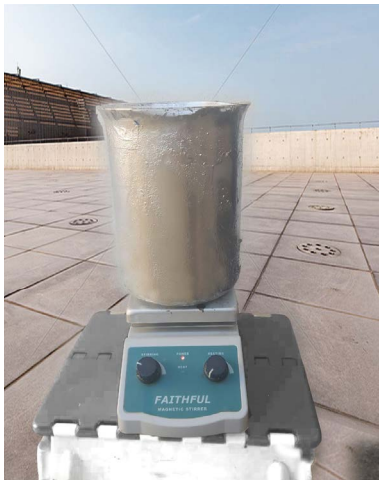

Fig. 1. Schematic of photo-oxidation process using solar source.

a stirrer type (MSH-300N, BOECO, Hamburg, Germany), first in the dark for 15 min to achieve primary adsorption equilibrium, and then start the solar photocatalyst reaction. Then at regular time intervals 10, 20, 30, 45, 60, and 90 min, samples were withdrawn, then centrifuged at 3,000 rpm for 15 min, and then analyzed by UV spectral analysis (Hitachi U-2001 spectrophotometer) at a λ_{max} of 420 nm. The removal performance of the target chemicals, on the other hand, was calculated using Eq. (8):

$$\text{Decolorization Efficiency} = \frac{C_o - C}{C_o} \times 100\% \tag{8}$$

where C_o and C represent the initial and final concentrations of the RY dye solution, respectively.

3. Response surface design

The experimental design by CCD method was conducted by the Design-Expert 13 program to 27 experiments to evaluate the impact of TiO_2, pH, H_2O_2, irradiation time, and RY dye concentration on the response variable (RY dye removal percentage). Table 1 shows the values of the independent variables and their variation limitations, which were established using related scientific literature as well as experimental results acquired in preliminary research using RY dye. The location of maximum removal, within the center point (the lowest and highest values), was marked as the center point (0) to obtain the repeatability of the method and to determine the experimental error. Furthermore, the second-order polynomial response equation, Eq. (9) can be used to correlate the independent and dependent variables [27].

$$\begin{aligned} Y = B_0 = {} & B_1X_1 + B_2X_2 + B_3X_3 + B_{11}X_{12} + B_{22}X_{22} \\ & + B_{33}X_{32} + B_{12}X_1X_2 + B_{23}X_2X_3 + B_{13}X_1X_3 \end{aligned} \tag{9}$$

where Y stands for a predicted response, x_i and x_j represent coded of variables, B_0; offset term, B_i, B_j, and B_{ij} represent first-order, quadratic, and interaction effects, and i and j for factor index numbers.

Table 1
Experimental range and levels of independent parameters

Factor	Name	Units	Low level	High level
A	pH	–	3	11
B	TiO_2	mg/L	25	100
C	H_2O_2	mg/L	100	700
D	Dye conc.	mg/L	25	100
E	Time	min	10	120

The data was analyzed using analysis of variance (ANOVA) to evaluate the interactive effects between the independent factors and responses in the process. The coefficients of the second-order model, which interpret the amount of removal of the researched parameters (responses), define the performance of independent variables. Multiple regressions were used to assess the research data. The coefficients were examined using analysis of variance, and the significance threshold was set at p 0.05. The determination coefficients (R^2) and adjusted-R^2 (R^2_{adj}) were used to control the model fitting quality, while the Fischer test was used to control the statistical significance (F-test) [28].

4. Results and discussion

According to the results, a small degradation was observed in the darkness after 15 min. However, the degradation efficiency increased when irradiation time was started. For that, the experimental design was performed for solar photocatalytic process results only.

4.1. Optimization representation

Table 2 lists all 78 numbers of the experimental design matrix, as well as responses based on experimental runs and estimated percent color reductions offered by CCD. Based on these findings, a polynomial model expressing the response function and the impact of the independent components is given as a second-order polynomial equation [Eq. (10)].

$$\begin{aligned} \text{Removal} = {} & 74.83 - 7.03A - 0.3870C - 15.78D + 8.16E \\ & - 2.13AE - 7.79A^2 + 4.08B^2 - 9.86C^2 \\ & - 11.07E^2 + 1.23BDE - 5.68A^2E + 3.06AE^2 \\ & - 3.28B^2E - 0.7841BE^2 - 1.55D^2E + 3.35DE^2 \\ & - 3.45C^3 + 4.08D^3 + 7.15E^3 + 2.62B^2E^2 + 4.16E^4 \end{aligned} \tag{10}$$

The actual and predicted RY dye removal percentage was given in Fig. 2, where the percentage removal efficiency of RY dye reached 96.02% which is significantly closer to the experimental removal percentage of 95%, this means there was a tendency for linear regression fit, and the model adequately explains the experimental range studied.

Table 2
Results of CCD with experimental and predicted values

Run	*A*: pH	*B*: TiO_2	*C*: H_2O_2	*D*: Dye conc.	*E*: Time	Response removal %	Predicted %
1	7	25	400	50	15	57	56.23
2	7	25	400	50	25	66	64.77
3	7	25	400	50	35	70	71.88
4	7	25	400	50	45	78	77.56
5	7	25	400	50	60	86	83.42
6	7	25	400	50	90	93	85.49
7	7	25	400	75	15	55	50.85
8	7	25	400	75	25	59	59.39
9	7	25	400	75	35	64	66.50
10	7	25	400	75	45	69	72.18
11	7	25	400	75	60	75	78.03
12	7	25	400	75	90	80	80.10
13	7	25	400	100	15	52	45.47
14	7	25	400	100	25	55	54.00
15	7	25	400	100	35	60	61.12
16	7	25	400	100	45	64	66.80
17	7	25	400	100	60	67	72.65
18	7	25	400	100	90	75	74.72
19	7	25	100	20	15	51	52.78
20	7	25	100	20	25	62	61.32
21	7	25	100	20	35	72	68.43
22	7	25	100	20	45	76	74.12
23	7	25	100	20	60	77	79.97
24	7	25	100	20	90	86	82.04
25	7	25	250	20	15	55	60.45
26	7	25	250	20	25	68	68.98
27	7	25	250	20	35	74	76.09
28	7	25	250	20	45	82	81.78
29	7	25	250	20	60	85	87.63
30	7	25	250	20	90	88	89.70
31	7	25	400	20	15	59	62.69
32	7	25	400	20	25	71	71.23
33	7	25	400	20	35	79	78.34
34	7	25	400	20	45	87	84.02
35	7	25	400	20	60	90	89.88
36	7	25	400	20	90	95	96.02
37	7	25	700	20	15	50	50.93
38	7	25	700	20	25	56	59.47
39	7	25	700	20	35	70	66.58
40	7	25	700	20	45	74	72.27
41	7	25	700	20	60	77	78.12
42	7	25	700	20	90	80	80.19
43	7	50	400	20	15	51	57.20
44	7	50	400	20	25	65	66
45	7	50	400	20	35	74	72.85
46	7	50	400	20	45	85	78.53
47	7	50	400	20	60	88	84.38
48	7	50	400	20	90	92	86.46
49	7	75	400	20	15	50	57.30
50	7	75	400	20	25	62	65.84

(Continued)

Table 2

Run	*A*: pH	*B*: TiO_2	*C*: H_2O_2	*D*: Dye conc.	*E*: Time	Response removal %	Predicted %
51	7	75	400	20	35	71	72.95
52	7	75	400	20	45	80	78.64
53	7	75	400	20	60	85	84.49
54	7	75	400	20	90	87	86.56
55	7	100	400	20	15	61	63.00
56	7	100	400	20	25	75	71.54
57	7	100	400	20	35	77	78.65
58	7	100	400	20	45	83	84.34
59	7	100	400	20	60	84	86.19
60	7	100	400	20	90	85	89.26
61	3	25	400	20	15	60	58.66
62	3	25	400	20	25	72	68.28
63	3	25	400	20	35	80	76.47
64	3	25	400	20	45	87	83.24
65	3	25	400	20	60	87	90.71
66	3	25	400	20	90	88	91.95
67	10	25	400	20	15	59	59.55
68	10	25	400	20	25	70	67.28
69	10	25	400	20	35	75	73.58
70	10	25	400	20	45	78	78.46
71	10	25	400	20	60	79	83.09
72	10	25	400	20	90	80	82.73
73	11	25	400	20	15	64	57.34
74	11	25	400	20	25	66	64.79
75	11	25	400	20	35	73	70.83
76	11	25	400	20	45	74	75.43
77	11	25	400	20	60	75	79.66
78	11	25	400	20	90	78	78.49

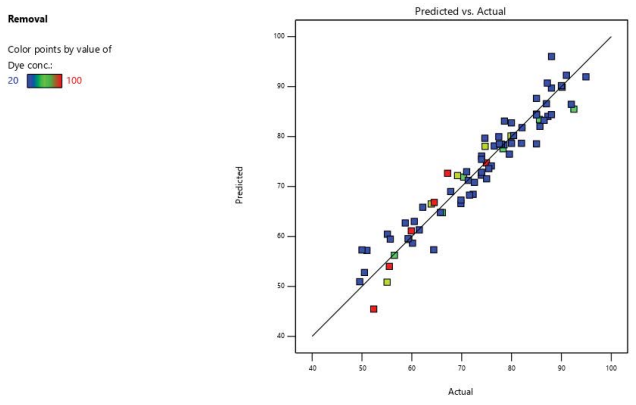

Fig. 2. Relation between predicted and actual data of RY decolorization.

4.2. Variance analysis

Table 3 shows the statistical significance of the quadratic model as determined by ANOVA. This table demonstrated that R^2 for the removal of RY dye was 0.9259, while (R^2_{adj}) was 0.9147 with an estimated difference of less than 0.2 suggesting good predictability of the model. In addition,

Table 3
ANOVA results for response quadratic models

Std. dev.	Mean	C.V. %	R^2	R^2_{adj}	R^2_{pre}	Adeq. precision
3.49	73.25	4.77	0.9259	0.9147	0.8846	38.2889

Table 3 shows the Adeq. precision ratio was 38.2889%, which means an adequate signal. In which Adeq. precision measures the ratio of signal to noise, and is desirable at a ratio > 4 [28,29]. However, Table 4 shows the statistical significance of the quadratic model as determined by ANOVA. The low *P*-value (0.0001) shows that the second-order quadratic model is significant for observed results [30]. In addition, the 82.46 *F*-value implies the significance of the model.

4.3. Response surface and contour plots for solar photocatalytic of RY dye removal

In order to understand the impact of different factors (pH, RY dye concentration, TiO_2 concentration, H_2O_2 concentration, and time) on RY dye removal efficiency, Fig. 3

Table 4
Analysis of variance (ANOVA) for RY dye removal percentage

Source	Sum of squares	df	Mean square	*F*-value	*P*-value	Characteristics
Model	1,0061.72	10	1,006.17	82.46	<0.0001	Significant
A-pH	324.30	1	324.30	26.58	<0.0001	
B-TiO_2	0.4160	1	0.4160	0.0341	0.8541	
C-H_2O_2	362.65	1	362.65	29.72	<0.0001	
D-Dye conc.	1,249.39	1	1,249.39	102.39	<0.0001	
E-Time	4,105.78	1	4,105.78	336.48	<0.0001	
AE	107.25	1	107.25	8.79	0.0042	
A^2	128.79	1	128.79	10.55	0.0018	
B^2	202.73	1	202.73	16.61	0.0001	
C^2	662.82	1	662.82	54.32	<0.0001	
E^2	1,304.84	1	1,304.84	106.93	<0.0001	
Residual	805.34	66	12.20			
Corr. Total	10,867.06	76				

contains both 3D surface and 2D contour plot. These figures were created by showing a function of two factors maintaining the other factor at a fixed level. Fig. 3a indicates the photocatalyst RY dye elimination vs. pH solution value and time while keeping other factors constant. It could be ascertained from this figure that the percentage removal increased by increasing the initial pH value from acidic condition to neutral (around 7). Further increases in initial pH (up to 10) show a significant decrease in the percentage removal. It is related to the ionization state of the surface according to the following reactions Eqs. (11) and (12), as well as to that of reactant dye and products such as acids and amines.

$$\mathrm{TiOH} + \mathrm{H^+} \leftrightarrow \mathrm{TiOH_2^+} \tag{11}$$

$$\mathrm{TiOH} + \mathrm{OH} \leftrightarrow \mathrm{OH^-} \leftrightarrow \mathrm{TiO} + \mathrm{H_2O} \tag{12}$$

The pH changes can thus influence the adsorption of dye molecules onto the TiO_2 surfaces, an important step for photocatalytic oxidation to take place [31].

Also, this figure present that there is a gradual increase in the efficiency of the photocatalytic process with the increase of exposure time until it reached 90 min. Further increase in contact time reduces the decolorization efficiency. This could be owing to the fact that radicals formed over a prolonged period of time are unstable in nature and disintegrate quickly [32].

The results of RY dye removal as a function of initial dye concentration 20, 50, 75, and 100 mg/L are present in Fig. 3b, which reveals that increasing the initial concentration of RY dye from 20 to 100 mg/L reduces the removal efficiency. At high dye concentrations, the catalytic surface is saturated with a large amount of dye adsorbed thereon, therefore it affects the catalytic activity of TiO_2, and reduces the path length of the photon-penetrating dye solution. Finally, dye molecules would be less transparent to light, and they may absorb large quantities of light, allowing less light to reach the catalyst and therefore limiting the creation of the OH radical. This observation is in line with the finding of Alahiane et al. [33].

The photocatalytic activities of the different concentrations of TiO_2 25, 50, 75, and 100 mg/L under direct sunlight were also evaluated and compared on the percentage of RY dye decolorization at the optimized values of RY dye (20 mg/L), and the pH of 7, and their results are shown in Fig. 3c the results reveal that the decolorization percentage decreased with increasing the catalyst weight above 25 mg/L. The increase in the catalyst weight above a certain limit reduces the light penetration and therefore reduces the photocatalytic activity [34].

Fig. 3d shows that the photocatalytic degradation rate of RY dye increased by increasing H_2O_2 concentration from 100 to 400 mg/L. This might be because the photo-dissociation of H_2O_2 produces the hydroxyl radical OH, which acts as a powerful oxidant and electron scavenger. Moreover increasing the concentration of hydrogen peroxide up to 700 mg/L decreases the photocatalytic degradation rate which could be contributed to the scavenging effect. However, the higher concentration of H_2O_2 inhibits catalytic activity as H_2O_2 is adsorbed onto TiO_2 [33]. Hydroxyl radicals are transformed into O_2, H_2O, and $^{\bullet}OOH$ radicals with weaker oxidizability, Eqs. (13) and (14) [35,36]:

$$\mathrm{H_2O_2} + {}^{\bullet}\mathrm{OH} \rightarrow {}^{\bullet}\mathrm{OOH} + \mathrm{H_2O} \tag{13}$$

$$^{\bullet}\mathrm{OOH} + {}^{\bullet}\mathrm{OH} \rightarrow \mathrm{O_2} + \mathrm{H_2} \tag{14}$$

4.4. Process optimization

In the numerical optimization, we choose the desired goal for each factor (pH, dye concentration, TiO_2 concentration, H_2O_2 concentration, and time) and response (RY dye removal). The possible goals are: maximize, minimize, target, within range, none (for responses only) and set to an exact value (factors only). A minimum and a maximum level must be provided for each parameter included. A weight can be assigned to each goal to adjust the shape of

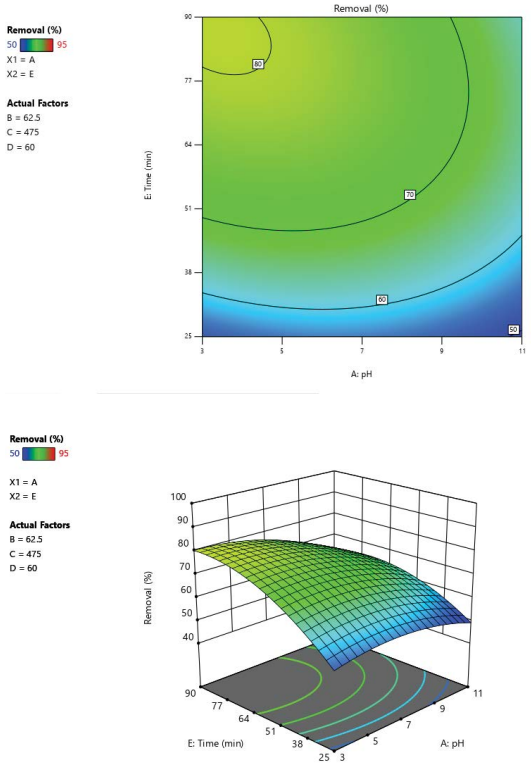

(a) pH

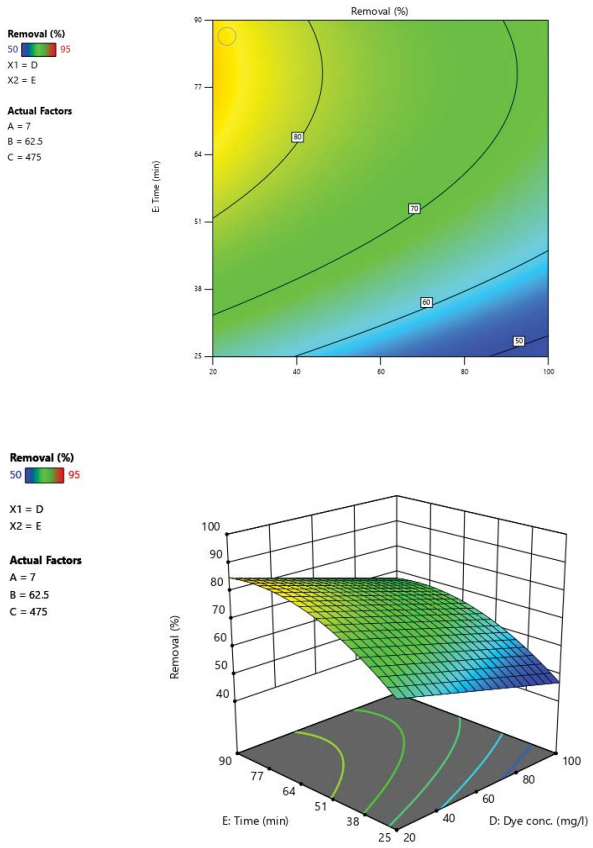

(b) RY dye concentration

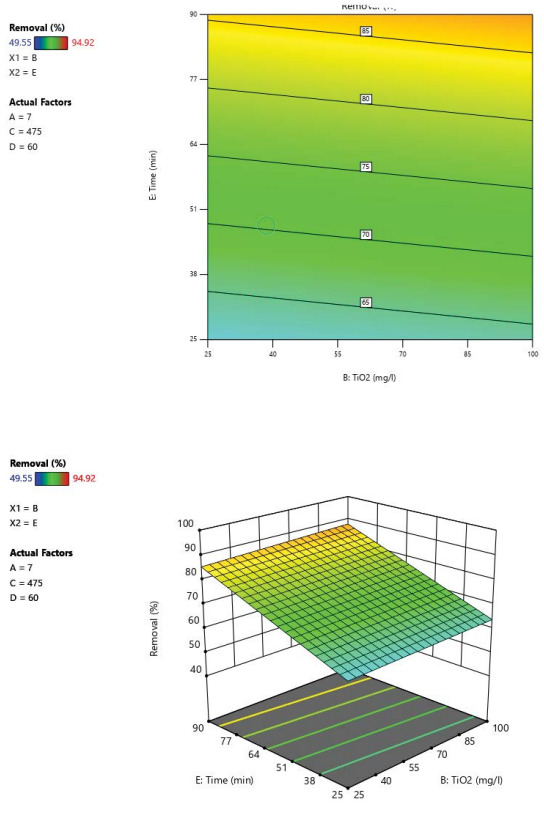

(c) TiO_2 concentration

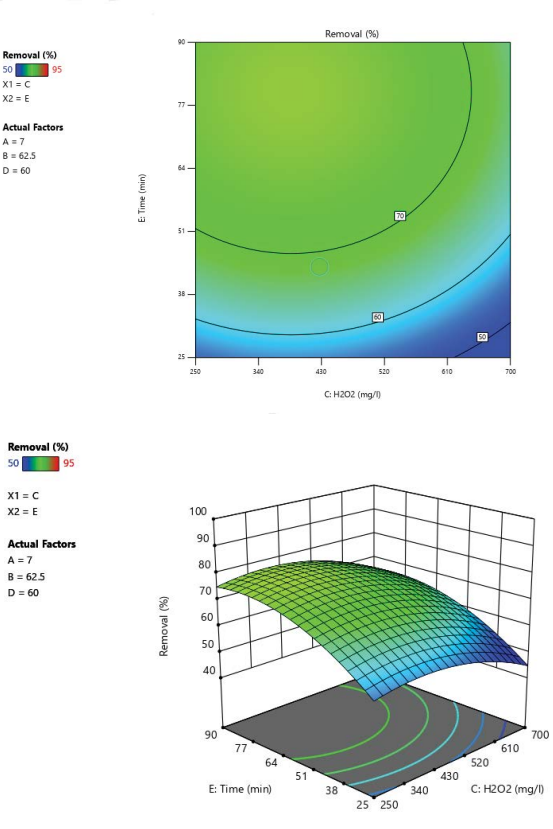

(d) H_2O_2 concentration

Fig. 3. 2D contour plots express and 3D surface plot of operating parameters on removal efficiency. (a) pH, (b) RY dye concentration, (c) TiO_2 concentration and (d) H_2O_2 concentration.

its particular desirability function. The goals are combined into an overall desirability function. Desirability is an objective function that ranges from zero outside of the limits to one at the goal. The program seeks to maximize this function. The goal-seeking begins at a random starting point and proceeds up the steepest slope to a maximum [37]. Fig. 4 shows the desirability profile of the projected response, which shows that the values of optimal circumstances for independent variables are as follows: (pH = 6.95294, TiO_2 = 25.5441 mg/L, H_2O_2 = 383.676 mg/L, time = 89.6176 min, and 20.9412 mg/L dye concentration), under these conditions the predicted value 91% and the desirability of 0.985, which indicates that the estimated function may express the desired conditions and the experimental model.

4.5. Kinetic degradation of RY

In order to investigate the degradation performance of solar photocatalytic processes for the degradation of RY dye from an aqueous solution, the kinetic analysis is essential for understanding the photodegradation process and reaction rate, which depend on the dynamic collaboration of RY dye and the nanocomposite surface. The reaction rate of heterogeneous catalytic reactions is usually typically described by a pseudo-first-order kinetics model and can be explained under the conditions of the Langmuir–Hinshelwood (L–H) kinetics model [38,39].

$$\ln\frac{C}{C_o} = k.t \tag{15}$$

where k is the observed pseudo-first-order reaction rate constant (1/min), C and C_o are the RY dye concentrations (mg/L) after exposure time t and the starting RY dye concentrations (mg/L), respectively, and t is the exposure period (min).

The kinetic results were achieved by plotting $\ln(C/C_o)$ as a function of t in the range of 0 to 90 min Fig. 5, and the results of k values and the regression coefficients (R^2) of the linear plot equations are present in Table 5. As it is clear from the results the constant degradation rate of k was reduced by increasing the initial concentration of RY dye, also the results show that the R^2 values of the RY dye removal reaction

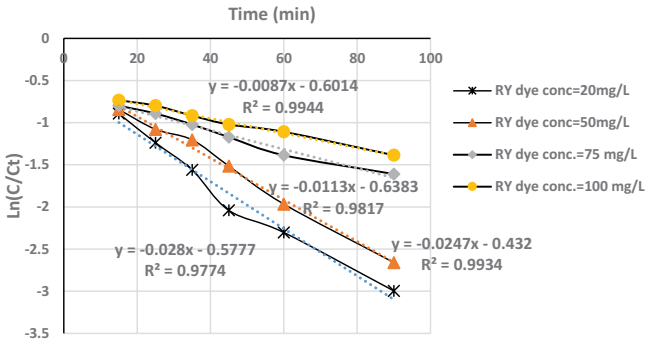

Fig. 5. Kinetics curve of pseudo-first-order equation for RY dye removal at different initial concentrations.

Table 5
Reaction rate parameters for RY dye decomposition in solar photocatalytic processes

RY dye conc.	Removal % at 90 min	First-order	
		K (min^{-1})	R^2
20	95	0.028	0.9774
50	93	0.0247	0.9934
75	80	0.0113	0.9817
100	75	0.0087	0.9944

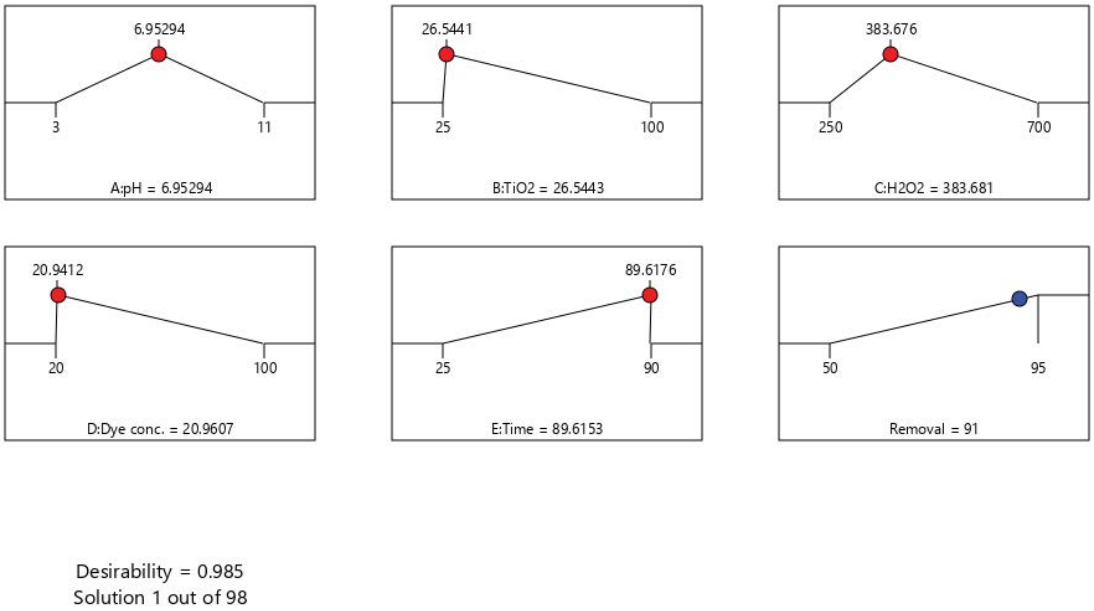

Fig. 4. Desirability profile of the predicted response.

curves at different dye concentrations were high (>90), this indicated that the reaction followed a pseudo-first-order kinetic model.

5. Conclusion

The results of this study demonstrated that a response surface methodology is a good tool for optimizing parameters found in the experimental data. A quadratic model was suggested as a good model for the prediction of RY dye removal. In addition, ANOVA analysis confirmed that pH (*A*), TiO_2 concentration (*B*), H_2O_2 concentration (*C*), RY dye concentration (*D*), and reaction time (*E*), square terms as well as interaction terms had significant effects on RY removal efficiency. The optimum conditions were found at: pH = 6.95294, TiO_2 = 25.5441 mg/L, H_2O_2 = 383.676 mg/L, time = 89.6176 min, and 20.9412 mg/L dye concentration. However, optimization of solar-induced photocatalytic degradation of RY dye from an aqueous solution by RSM resulted in 91% lead removal. The findings proved a good agreement between the experimental data and the predicted equation. It is also worth highlighting that the RY dye removal appears to follow pseudo-first-order kinetics and that the rate constant is inversely proportional to the pollutant's initial concentration level. Therefore, the RSM can be proposed as a useful tool for the optimization of dye wastewater treatment using solar-induced photocatalytic processes.

Acknowledgments

The authors express their gratitude to the University of Baghdad (Baghdad, Iraq) for providing facilities for this research.

Financial and ethical disclosures

This research did not receive any specific grant from funding in the public, commercial, or not-for-profit sectors.

Author's contribution

All authors have participated in (a) conception and design, or analysis and interpretation of the data; (b) drafting the article or revising it critically for important intellectual content, and (c) approval of the final version.

Conflict of interest

This manuscript has not been submitted to, nor is it under review at, another journal or other publishing venue.

The authors have no affiliation with any organization with a direct or indirect financial interest in the subject matter discussed in the manuscript.

On behalf of all authors, the corresponding author states that there is no conflict of interest.

Data availability statements

The datasets generated during and/or analyzed during the current study are available from the corresponding author upon reasonable request.

References

[1] R. Venkataraghavan, R. Thiruchelvi, D. Sharmila, Statistical optimization of textile dye effluent adsorption by *Gracilaria edulis* using Plackett-Burman design and response surface methodology, Heliyon, 6 (2020) e05219, doi: 10.1016/j.heliyon.2020.e05219.

[2] B. Lellis, C.Z. Fávaro-Polonio, J.A. Pamphile, J.C. Polonio, Effects of textile dyes on health and the environment and bioremediation potential of living organisms, Biotechnol. Res. Innovation, 3 (2019) 275–290.

[3] S. Ledakowicz, K. Paździor, Recent achievements in dyes removal focused on advanced oxidation processes integrated with biological methods, Molecules, 26 (2021) 870, doi: 10.3390/molecules26040870.

[4] A.R. Tehrani-Bagha, F.L. Amini, Decolorization of a reactive dye by UV-enhanced ozonation, Prog. Color Colorants Coat., 3 (2010) 1–8.

[5] A.I. Alwared, T.J. Al-Musawi, L.F. Muhaisn, A.A. Mohammed, The biosorption of reactive red dye onto orange peel waste: a study on the isotherm and kinetic processes and sensitivity analysis using the artificial neural network approach, Environ. Sci. Pollut. Res., 28 (2021) 2848–2859.

[6] L. Brinza, A.E. Maftei, S. Tascu, F. Brinza, M. Neamtu, Advanced removal of reactive yellow 84 azo dye using functionalised amorphous calcium carbonates as adsorbent, Sci. Rep., 12 (2022) 3112, doi: 10.1038/s41598-022-07134-2.

[7] H.N.J. Hoong, N. Ismail, Removal of dye in wastewater by adsorption-coagulation combined system with *Hibiscus sabdariffa* as the coagulant, MATEC Web Conf., 152 (2018) 01008, doi: 10.1051/matecconf/201815201008.

[8] E.R. Salmani, G. Akram, A. Saeid, D. Maryam, N. Nasrin, Removal of reactive Red 141 dye from synthetic wastewater by electrocoagulation process: investigation of operational parameters, Iran. J. Health Saf. Environ., 3 (2016) 403.

[9] S.A. Mousavi, S. Nazari, Applying response surface methodology to optimize the Fenton oxidation process in the removal of Reactive Red 2, Pol. J. Environ. Stud., 26 (2017) 765–772.

[10] I. Sabah, A.I. Alwared, Adsorption of Congo red dye from aqueous solutions by wheat husk, Univ. Baghdad Eng. J., 25 (2019) 72–84.

[11] Y.A. Mustafa, A.B. Hassan, Treatment of wastewater contaminated with pesticide (Alachlor) by solar enhanced advanced oxidation processes, J. Eng., 21 (2015) 130–144.

[12] A.N. Mohammed, I.A. Alwared, S.M. Salman, Photocatalytic degradation of reactive yellow dye in wastewater using H_2O_2/TiO_2/UV technique, Iraqi J. Chem. Pet. Eng., 21 (2020) 15–21.

[13] R.H. Al-Anbari, A.H.M. Jawad Al-Obaidy, E. Abed, Mohammed, Solar photocatalytic of reactive blue dye in aqueous suspension of V_2O_5, Eng. Technol. J., 35 (2017) 1–8.

[14] H.-w. Wang, X. Fang, Y.-c. Wan, J. Zhan, Z.-j. Wang, H. Liu, Visible-light-induced $NiCo_2O_4$@Co_3O_4 core/shell heterojunction photocatalysts for efficient removal of organic dyes, J. Cent. South Univ., 28 (2021) 3040–3049.

[15] F. Kargar, A. Bemani, M.H. Sayadi, N. Ahmadpour, Synthesis of modified beta bismuth oxide by titanium oxide and highly efficient solar photocatalytic properties on hydroxychloroquine degradation and pathways, J. Photochem. Photobiol., A, 419 (2021) 113453, doi: 10.1016/j.jphotochem.2021.113453.

[16] I. Barba-Nieto, K.C. Christoforidis, M. Fernández-García, A. Kubacka, Promoting H_2 photoproduction of TiO_2-based materials by surface decoration with Pt nanoparticles and SnS_2 nanoplatelets, Appl. Catal., B, 277 (2020) 119246, doi: 10.1016/j.apcatb.2020.119246.

[17] H.B. Hadjltaief, M.E. Galvez, M.B. Zina, P.D. Costa, TiO_2/clay as a heterogeneous catalyst in photocatalytic/photochemical oxidation of anionic reactive blue 19, Arabian J. Chem., 12 (2014) 1454–1462.

[18] O. Benhabiles, N. Chekir, D. Tassalit, N.K. Merzouk, M. Ghenna, A. Abdessemed, R. Issaadi, Solar Photocatalytic Degradation of Tartrazine via Immobilized Catalyst, A. Kallel, M. Ksibi, H. Ben Dhia, N. Khélifi, Eds., Recent Advances in Environmental

Science from the Euro-Mediterranean and Surrounding Regions, Proceedings of Euro-Mediterranean Conference for Environmental Integration (EMCEI-1), Tunisia 2017, 2018.
[19] S. Dutta, A. Ghosh, S.Ch. Moi, R. Saha, Application of response surface methodology for optimization of reactive azo dye degradation process by Fenton's oxidation, Int. J. Environ. Sci. Dev., 6 (2015), doi: 10.7763/IJESD.2015.V6.705.
[20] N. Sultana, S.M. Zakir Hossain, M. Ezzudin Mohammed, M.F. Irfan, B. Haq, M.O. Faruque, S.A. Razzak, M.M. Hossain, Experimental study and parameters optimization of microalgae based heavy metals removal process using a hybrid response surface methodology-crow search algorithm, Sci. Rep., 10 (2020) 15068, doi: 10.1038/s41598-020-72236-8.
[21] R. Shokri, R.J. Yengejeh, A.A. Babaei, E. Derikvand, A. Almasi, UV activation of hydrogen peroxide for removal of azithromycin antibiotic from aqueous solution: determination of optimum conditions by response surface methodology, Toxin Rev., 39 (2019) 284–291.
[22] C. Wang, H. Wang, G. Gu, Ultrasound-assisted xanthation of cellulose from lignocellulosic biomass optimized by response surface methodology for Pb(II) sorption, Carbohydr. Polym., 182 (2018) 21–28.
[23] Y.S. Zhang, H. Jiang, K. Wang, H. Wang, C. Wang, Green flotation of polyethylene terephthalate and polyvinyl chloride assisted by surface modification of selective $CaCO_3$ coating, J. Cleaner Prod., 242 (2020) 118441, doi: 10.1016/j.jclepro.2019.118441.
[24] A. Shokri, P. Daraei, S. Zereshki, Water decolorization using waste cooking oil: an optimized green emulsion liquid membrane by RSM, J. Water Process Eng., 33 (2020) 101021, doi: 10.1016/j.jwpe.2019.101021.
[25] F.A. Sulaiman, A.I. Alwared, Green synthesis of TiO_2 using *Ocimum basilicum* leaf extract and its application, Desal. Water Treat., 262 (2022) 312–322.
[26] M. Zaier, L. Vidal, S. Hajjar-Garreau, L. Balan, Generating highly reflective and conductive metal layers through a light-assisted synthesis and assembling of silver nanoparticles in a polymer matrix, Sci. Rep., 7 (2017) 12410, doi: 10.1038/s41598-017-12617-8.
[27] S. Chakrabarti, B.K. Dutta, Photocatalytic degradation of model textile dyes in wastewater using ZnO as semiconductor catalyst, J. Hazard. Mater., 112 (2004) 269–278.
[28] M. Darvishmotevalli, A. Zarei, M. Moradnia, M. Noorisepehr, H. Mohammadi, Optimization of saline wastewater treatment using electrochemical oxidation process: prediction by RSM method, Methods X, 6 (2019) 1101–1113.
[29] S.A. Mousavi, S. Ibrahim, Application of response surface methodology (RSM) for analyzing and modeling of nitrification process using sequencing batch reactors, Desal. Water Treat., 57 (2016) 5730–5739.
[30] D. Ozturk, T. Şahan, T. Bayram, A. Erkuş, Application of response surface methodology (RSM) to optimize the adsorption conditions of cationic basic yellow 2 onto pumice samples as a new adsorbent, Fresenius Environ. Bull., 26 (2017) 3285–3292.
[31] A. Giwa, P.O. Nkeonye, K.A. Bello, E.G. Kolawole, A.M.F. Oliveira Campos, Solar photocatalytic degradation of reactive yellow 81 and Reactive Violet 1 in aqueous solution containing semiconductor oxides, Int. J. Appl. Sci. Technol., 2 (2012) 90–105.
[32] K. Bukhari, N. Ahmad, I.R. Sheikh, T.M. Akram, Effects of different parameters on photocatalytic oxidation of slaughterhouse wastewater using TiO_2 and silver-doped TiO_2 nanoparticles, Pol. J. Environ., 28 (2018) 1591–1600.
[33] S. Alahiane, S. Qourzal, M. El Ouardi, A. Abaamrane, A. Assabbane, Factors influencing the photocatalytic degradation of reactive yellow 145 by TiO_2-coated non-woven fibers, Am. J. Anal. Chem., 5 (2014) 445–454.
[34] K. Thamaraiselvi, T. Sivakumar, A. Brindha, E. Elangovan, Photocatalytic degradation of reactive dyes over titanates, J. Nanosci. Nanotechnol., 19 (2019) 2087–2098.
[35] C. Wang, R. Sun, R. Huang, H. Wang, Superior Fenton-like degradation of tetracycline by iron loaded graphitic carbon derived from microplastics: synthesis, catalytic performance, and mechanism, Sep. Purif. Technol., 270 (2021) 118773, doi: 10.1016/j.seppur.2021.118773.
[36] B.-y. Fan, H.-b. Liu, Z.-h. Wang, Y.-w. Zhao, S. Yang, S.-y. Lyu, A. Xing, J. Zhang, H. Li, X.-y. Liu, Ferroelectric polarization-enhanced photocatalytic performance of heterostructured $BaTiO_3$@TiO_2 via interface engineering, J. Cent. South Univ., 28 (2021) 3778–3789.
[37] M. Amini, H. Younesi, N. Bahramifar, A.A.Z. Lorestani, F. Ghorbani, A. Daneshi, M. Sharifzadeh, Application of response surface methodology for optimization of lead biosorption in an aqueous solution by *Aspergillus niger*, J. Hazard. Mater., 154 (2008) 694–702.
[38] K. Swaminathan, S. Sandhya, S.A. Carmalin, K. Pachhade, V.Y. Subrahmanyam, Decolorization and degradation of H-acid and other dyes using ferrous–hydrogen peroxide system, Chemosphere, 50 (2003) 619–625.
[39] N. Nasseh, L. Taghavi, B. Barikbin, M.A. Nasseri, Synthesis and characterizations of a novel $FeNi_3/SiO_2/CuS$ magnetic nanocomposite for photocatalytic degradation of tetracycline in simulated wastewater, J. Cleaner Prod., 179 (2018) 42–54.